

# Introduction to Micromechatronics

K. Uchino, International Center for Actuators and Transducers, Penn State University  
University Park, PA 16802, USA

## 1. THE NEED FOR NEW ACTUATORS

An *actuator* is a transducer that transforms drive energy into a mechanical displacement or force. The demand for new actuators has increased significantly in recent years especially for *positioner*, *mechanical damper*, and *miniature motor* applications. These devices are used in a variety of fields such as optics, astronomy, fluid control, and precision machining.

Sub-micrometer fabrication, common in the production of electronic chip elements, is also becoming important in mechanical engineering. The trends depicted in Figure 1 show how machining accuracy has improved over the years.<sup>1</sup> One of the primary reasons for the improved accuracy is the development of more precise position sensors. Sensors utilizing lasers can easily detect nanometer scale displacements. This could be regarded as another instance of "the chicken or the egg" issue, however, as the fabrication of such precise optical instruments can only be achieved with the submicrometer machining equipment the sensors are designed to monitor.

In an actual machining apparatus comprised of translational components (the joints) and rotating components (the gears and motor) error due to backlash will occur. Machine vibration will also lead to unavoidable position fluctuations. Furthermore, the deformations due to machining stress and thermal expansion also cannot be ignored. The need for submicron displacement positioners to improve cutting accuracy is apparent. One example is a prototype for a lathe machine that uses a ceramic multilayer actuator and can achieve cutting accuracy of  $0.01\mu\text{m}$ .<sup>2</sup>

The concept of "*adaptive optics*" has been applied in the development of sophisticated new optical systems. Earlier systems were generally designed such that parameters like position, angle, or the focal lengths of mirror and lens components remained essentially fixed during operation. Newer systems incorporating adaptive optical elements respond to a variety of conditions to essentially adjust the system parameters to maintain optimum operation. The original "lidar" system (a radar system utilizing light waves) was designed to be used on the NASA space shuttle for monitoring the surface of the earth.<sup>3</sup> A laser beam is projected towards the earth's surface, and the reflected light is received by a reflection telescope, amplified by a photomultiplier, and the resulting signal is processed to produce an image. The vibration noise and temperature fluctuations of the shuttle make it difficult for a sharp image to be obtained, however, and the use of a responsive positioner was considered to compensate for the detrimental effects.

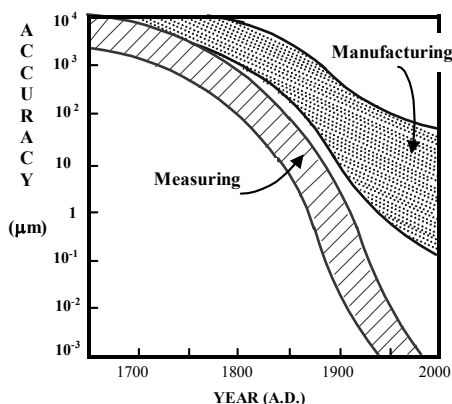


**Figure 1** Obtainable accuracies in manufacturing and measurement over time. Note that current accuracies tend to be on the micrometer and nanometer scales, respectively.

## Report Documentation Page

*Form Approved*  
*OMB No. 0704-0188*

Public reporting burden for the collection of information is estimated to average 1 hour per response, including the time for reviewing instructions, searching existing data sources, gathering and maintaining the data needed, and completing and reviewing the collection of information. Send comments regarding this burden estimate or any other aspect of this collection of information, including suggestions for reducing this burden, to Washington Headquarters Services, Directorate for Information Operations and Reports, 1215 Jefferson Davis Highway, Suite 1204, Arlington VA 22202-4302. Respondents should be aware that notwithstanding any other provision of law, no person shall be subject to a penalty for failing to comply with a collection of information if it does not display a currently valid OMB control number.

1. REPORT DATE <b>00 JUN 2003</b>	2. REPORT TYPE <b>N/A</b>	3. DATES COVERED <b>-</b>	
4. TITLE AND SUBTITLE <b>Introduction to Micromechatronics</b>		5a. CONTRACT NUMBER	
		5b. GRANT NUMBER	
		5c. PROGRAM ELEMENT NUMBER	
6. AUTHOR(S)		5d. PROJECT NUMBER	
		5e. TASK NUMBER	
		5f. WORK UNIT NUMBER	
7. PERFORMING ORGANIZATION NAME(S) AND ADDRESS(ES) <b>International Center for Actuators and Transducers, Penn State University University Park, PA 16802, USA</b>		8. PERFORMING ORGANIZATION REPORT NUMBER	
9. SPONSORING/MONITORING AGENCY NAME(S) AND ADDRESS(ES)		10. SPONSOR/MONITOR'S ACRONYM(S)	
		11. SPONSOR/MONITOR'S REPORT NUMBER(S)	
12. DISTRIBUTION/AVAILABILITY STATEMENT <b>Approved for public release, distribution unlimited</b>			
13. SUPPLEMENTARY NOTES <b>See also ADM001697, ARO-44924.1-EG-CF, International Conference on Intelligent Materials (5th) (Smart Systems &amp; Nanotechnology)., The original document contains color images.</b>			
14. ABSTRACT			
15. SUBJECT TERMS			
16. SECURITY CLASSIFICATION OF:			17. LIMITATION OF ABSTRACT
a. REPORT <b>unclassified</b>	b. ABSTRACT <b>unclassified</b>	c. THIS PAGE <b>unclassified</b>	<b>UU</b>
			18. NUMBER OF PAGES <b>26</b>
			19a. NAME OF RESPONSIBLE PERSON

Active and passive vibration suppression by means of piezoelectric devices is also promising technology for use in space structures and military and commercial vehicles. Mechanical vibration in a structure traveling through the vacuum of space is not readily damped and a 10 m long array of solar panels can be severely damaged simply by the repeated impact of space dust with the structure. Active dampers using shape memory alloys or piezoelectric ceramics are currently under investigation to remedy this type of problem. A variety of *smart skins* designed for military tanks or submarines are illustrated in Figure 2. A signal is generated in the sensitive skin with perhaps the impact of a missile on the tank or the complex forces applied to a submarine through turbulent flow, which is fed back to an actuator. The actuator responds by changing its shape to effectively minimize the impact damage on the tank (*structure protection*) or the drag force on the submarine.

The demand for other applications in the field of mechanical engineering is also increasing rapidly. One important class of devices that meets these demands is the "*solid-state motor*." Market research focused on just office equipment needs, such as printers and floppy disk drives, indicates that tiny motors smaller than 1 cm will be in increasing demand over the next ten years. Conventional electromagnetic motor designs, however, do not provide sufficient energy efficiency for these applications. Piezoelectric *ultrasonic motors*, whose efficiency is insensitive to size, are superior to the conventional devices when motors of millimeter size are required.

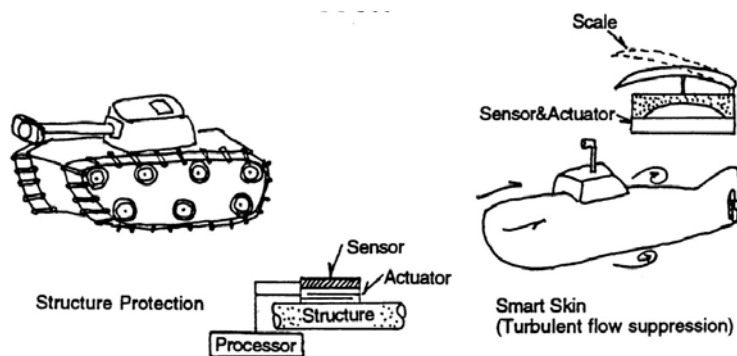


**Figure 2** Smart skin structures for military tanks and submarines.

## 2. CONVENTIONAL METHODS FOR MICROPOSITIONING

A classification of actuators, is presented in Table 1. This classification is based on the features of the actuator that relate to micropositioning controllability. Electrically controlled types are generally preferred for applications where miniature devices are needed. A few of the relevant specifications for the solid-state actuators included in this classification also appear in the table. Compared with conventional devices, the new principle actuators provide much quicker response, smaller size, higher resolution, and a higher power-to-weight ratio.

Conventional methods for micropositioning usually include displacement reduction mechanisms to suppress mechanical backlash, which are categorized into three general groups: (1) oil/air pressure displacement reduction, (2) the electromagnetic rotary motor with a gear, and (3) the voice coil motor.<sup>4</sup> A brief description of each follows.

### (1) Oil Pressure Type Displacement Reduction Mechanism

Changing the diameter of an oil-filled cylinder as illustrated in Figure 3 effectively reduces the resulting displacement at the output. Devices utilizing this oil pressure mechanism are generally large and have slow responses. Transducers of this type are sometimes used in the reverse mode for amplifying the displacement produced by a solid-state actuator.

### (2) Combination of a Motor and a Displacement Reduction Mechanism

Screw transfer mechanisms are typically used when the moving distance is long (see Figure 4). Using very precise ball screws, positioning accuracy of less than 5  $\mu\text{m}$  can be obtained for a 100 mm motion. When higher accuracies are required, additional displacement reduction mechanisms are necessary.

**Table 1** Displacement characteristics of various types of actuators.

Drive	Device	Displacement	Accuracy	Torque/ Generative Force	Response Time
Air pressure	Motor	Rotation	degrees	50 Nm	10 sec
	Cylinder	100 mm	100 $\mu\text{m}$	$10^{-1}$ N/mm <sup>2</sup>	10 sec
Oil pressure	Motor	Rotation	degrees	100 Nm	1 sec
	Cylinder	1000 mm	10 $\mu\text{m}$	100 N/mm <sup>2</sup>	1 sec
Electricity	AC Servo Motor	Rotation	minutes	30 Nm	100 msec
	DC Servo Motor	Rotation	minutes	200 Nm	10 msec
	Stepper Motor	1000 mm	10 $\mu\text{m}$	300 N	100 msec
	Voice Coil Motor	1 mm	0.1 $\mu\text{m}$	300 N	1 msec
	New Piezoelectric	100 $\mu\text{m}$	0.01 $\mu\text{m}$	30 N/mm <sup>2</sup>	0.1 msec
	Magnetostrictor	100 $\mu\text{m}$	0.01 $\mu\text{m}$	100 N/mm <sup>2</sup>	0.1 msec
	Ultrasonic Motor (piezoelectric)	Rotation	minutes	1 Nm	1 msec

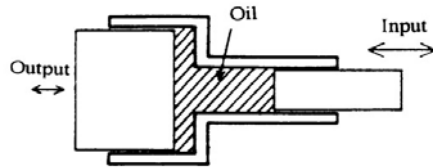


**Figure 3** Schematic representation of an oil pressure displacement reduction mechanism.

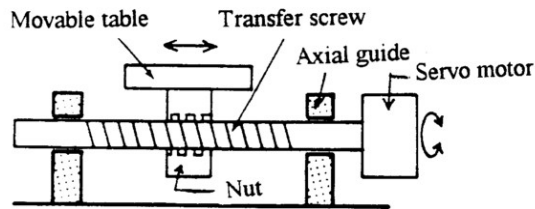


**Figure 4** Illustration of a screw positioning mechanism.

There are several other commonly used displacement reduction mechanisms. The mechanisms highlighted in Figure 5 illustrate the action of a spring constant difference, a hinge lever, and a wedge. The combination of a motor with a ball screw or a displacement reduction mechanism has the advantages of quick response, a substantial generative force, and good controllability, but is generally difficult to fabricate in miniature form due to its structural complexity. In addition, the manufacturing tolerances of a typical transfer screw tend to promote backlash in positioning even when displacement reduction mechanisms are implemented.

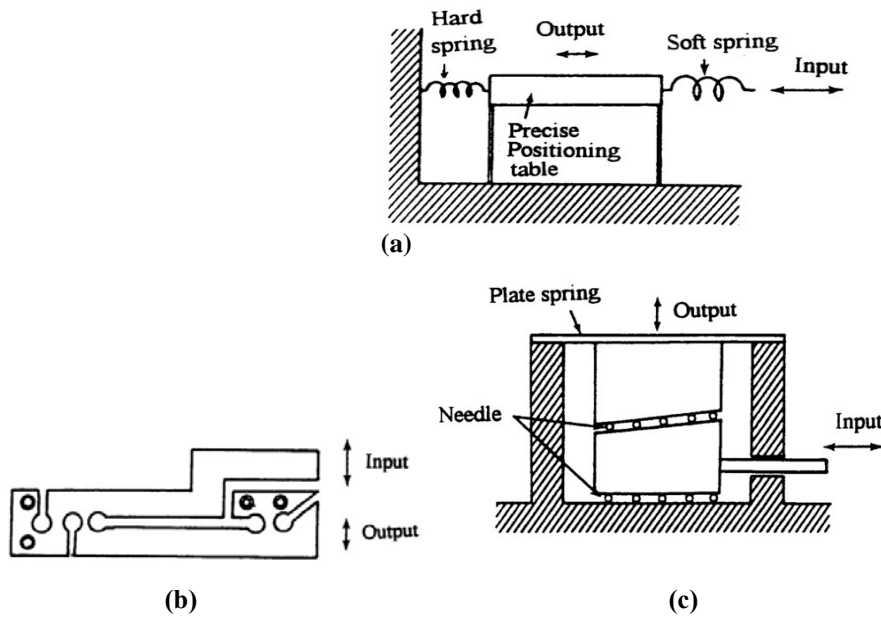


**Figure 5** Illustrations of several displacement reduction mechanisms utilizing the action of: (a) a spring constant difference, (b) a hinge lever, and (c) a wedge.

The minimum size of an electromagnetic motor is generally limited to about 1 cm, as motors smaller than this will not provide adequate torque and efficiency. One of the smallest electromagnetic motors to be fabricated is shown in Figure 6.<sup>5</sup> A micromotor with a diameter of 1.9 mm typically generates a torque of only 7.5  $\mu\text{Nm}$  and rotational speeds of 100,000 rpm. An optional microgearbox with a reduction ratio of 47 can be used with this motor so that the drive can deliver an enhanced torque of up to 300  $\mu\text{Nm}$ . Use of this gearbox, however, reduces the efficiency of the motor significantly. Further, as the size of electromagnetic motor is reduced the winding wire thickness must also be reduced, which leads to a significant increase in the electrical resistance and Joule heating.

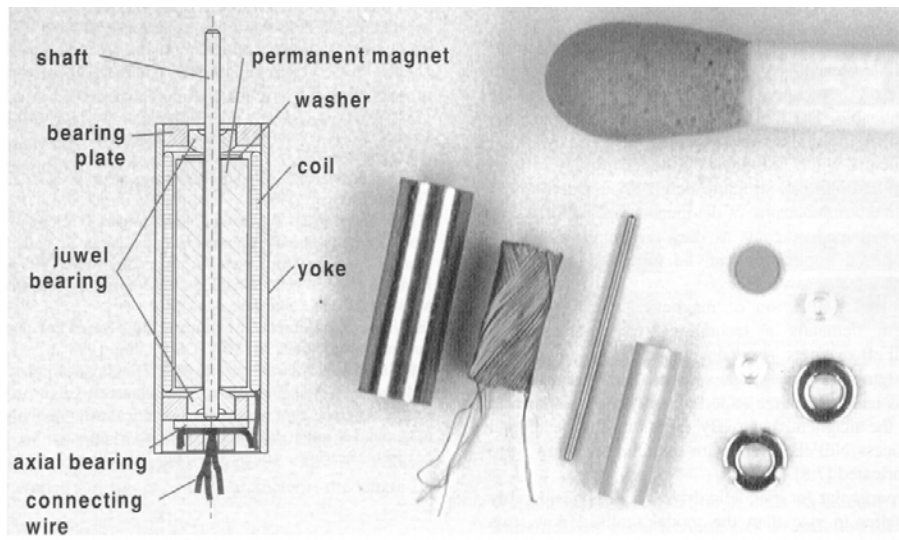


**Figure 6** An electromagnetic micromotor with a diameter of 1.9 mm, developed by the Institute of Microtechnique, Mainz GmbH.<sup>5</sup>

### (3) Voice Coil Motors

The structure of a voice coil motor is shown schematically in Figure 7. Among the three displacement control devices described here, this motor achieves the most precise positioning. It requires relatively large input electrical energy, however, has a slow response, and produces rather low generative forces.

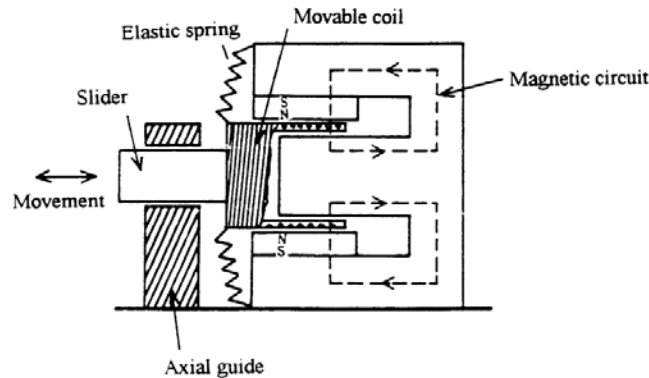


Figure 7 Schematic representation of a voice coil motor.

The search for new solid-state actuators that do not use springs or gear mechanisms has thus developed in recent years to more effectively and reliably provide the displacements required for micropositioning applications. A review of the current technology related to state-of-the-art solid-state actuators is presented in the next section.

## 3. AN OVERVIEW OF SOLID-STATE ACTUATORS

### (1) Smart Actuators

Let us now consider the "smartness" of a material. The various properties relating the input parameters of electric field, magnetic field, stress, heat and light with the output parameters, charge/current, magnetization, strain, temperature and light are listed in Table 2. Conducting and elastic materials, which generate current and strain outputs, respectively, with input, voltage or stress (diagonal couplings), are sometimes referred to as "*trivial*" materials. High temperature superconducting ceramics are also considered trivial materials in this sense, but the figure of merit (electrical conductivity) exhibited by some new compositions has been exceptionally high in recent years making them especially newsworthy.

On the other hand, pyroelectric and piezoelectric materials, which generate an electric field with the input of heat and stress, respectively, are called *smart materials*. These off-diagonal couplings have corresponding converse effects, the electrocaloric and converse piezoelectric effects, so that both "sensing" and "actuating" functions can be realized in the same material. One example is a tooth brace made of a shape memory (super-elastic) alloy. A temperature dependent phase transition in the material responds to variations in the oral temperature, thereby generating a constant stress on the tooth.

"Intelligent" materials must possess a "drive/control" or "processing" function, which is adaptive to changes in environmental conditions in addition to their actuator and sensing functions. Photostrictive actuators belong to this category. Some ferroelectrics generate a high voltage when illuminated (the *photovoltaic effect*). Since the ferroelectric is also piezoelectric, the photovoltage produced will induce a strain in the crystal. Hence, this type of material generates a drive voltage dependent on the intensity of the incident light, which actuates a mechanical response. The self-repairing nature of partially stabilized zirconia can also be considered an intelligent response. Here, the material responds to the stress concentrations produced with the initial development of the microcrack

(sensing) by undergoing a local phase transformation in order to reduce the concentrated stress (control) and stop the propagation of the crack (actuation).

If one could incorporate a somewhat more sophisticated mechanism for making complex decisions to its “intelligence,” a *wise material* might be created. Such a material might be designed to determine that “this response may cause harm” or “this action will lead to environmental destruction,” and respond accordingly. It would be desirable to incorporate such fail-safe mechanisms in actuator devices and systems. A system so equipped would be able to monitor for and detect the symptoms of wear or damage so as to shut itself down safely before serious damage or an accident occurred.

**Table 2** Various basic and cross-coupled properties of materials.

OUTPUT INPUT	CHARGE/ CURRENT	MAGNETI- ZATION	STRAIN	TEMPERATURE	LIGHT
ELECTRIC FIELD	Permittivity Conductivity	Electromagnetic Effect	Converse Piezoelectric Effect	Electrocaloric Effect	Electrooptic Effect
MAGNETIC FIELD	Magnetolectric Effect	Permeability	Magnetostriction	Magnetocaloric Effect	Magnetooptic Effect
STRESS	Piezoelectric Effect	Piezomagnetic Effect	Elastic Constants	****	Photoelastic Effect
HEAT	Pyroelectric Effect	****	Thermal Expansion	Specific Heat	****
LIGHT	Photovoltaic Effect	****	Photostriction	****	Refractive Index

**Diagonal Coupling:**       **Sensor:**

**Off-Diagonal Coupling:**      **Smart Material**      **Actuator:**

## (2) New Actuators

Actuators that operate by means of a mechanism different from those found in the conventional AC/DC electromagnetic motors and oil/air pressure actuators are generally classified as “*new actuators*.” Some recently developed new actuators are classified in Table 3 in terms of input parameter. Note that most of the new actuators are made from some type of solid material with properties specifically tailored to optimize the desired actuating function. That is why these actuators are sometimes referred to as just *solid-state actuators*. We will examine in this section some of the most popular and useful types of materials utilized for this class of actuators and their associated properties.

The displacement of an actuator element must be controllable by changes in an external parameter such as temperature, magnetic field or electric field. Actuators activated by changes in temperature generally operate through the *thermal expansion* or dilatation associated with a phase transition, such as the ferroelectric and martensitic transformations. *Shape memory alloys*, such as Nitinol, are of this type. Magnetostrictive materials, such as Terfenol-D, respond to changes in an applied magnetic field. *Piezoelectric* and *electrostrictive* materials are typically used in electric field-controlled actuators. In addition to these, we will consider silicon-based micro-electro-mechanical-systems (MEMS), polymer artificial muscles, light activated actuators (for which the displacements occur through the photostrictive effect or a photoinduced phase transformation), and electro/magnetorheological fluids.

**Table 3** New actuators classified in terms of input parameter.

<b>Input Parameter</b>	<b>Actuator Type/Device</b>
Electric Field	Piezoelectric/Electrostrictive Electrostatic (Silicon MEMS) Electrorheological Fluid
Magnetic Field	Magnetostrictive Magnetorheological Fluid
Stress	Rubbertuator
Heat	Shape Memory Alloy Bubble Jet
Light	Photostrictive Laser Light Manipulator
Chemical	Mechanochemical Metal-Hydrate

The desired general features for an actuator element include:

- 1) large displacement (sensitivity = displacement/ driving power),
- 2) good positioning reproducibility (low hysteresis),
- 3) quick response,
- 4) stable temperature characteristics,
- 5) low driving energy,
- 6) large generative force and failure strength,
- 7) small size and light weight,
- 8) low degradation/aging in usage,
- 9) minimal detrimental environmental effects (mechanical noise, electro-magnetic noise, heat generation, etc.).

### **(3) MEMS: MicroElectromechanical Systems**

Silicon has become almost synonymous with integrated electronic circuitry. Due to its favorable mechanical properties, silicon can also be micromachined to create microelectromechanical systems (MEMS).<sup>6</sup> The techniques for micromachining silicon have developed over the past ten years in a variety of industries for a wide range of applications. Pressure and acceleration sensors are produced for application in medical instrumentation and automobiles. One important example is the acceleration sensor used to trigger an air bag in an automobile crash. The generative force/displacement levels produced by MEMS devices are, however, generally too small to be useful for many actuator applications.

In *bulk micromachining*, mechanical structures are fabricated directly on a silicon wafer by selectively removing wafer material. Etching is the primary technique for bulk micromachining, and is either isotropic, anisotropic, or a combination of the two states. The etch rate for anisotropic etching depends on the crystallographic orientation; for example, an anisotropy ratio of 100:1 is possible in the <100> direction relative to the <111> direction. Etch processes can be made selective by using dopants (heavily doped regions etch slowly), or may be halted electrochemically (etching stops in a region of different polarity in a biased p-n junction). After the etching process is complete, the silicon wafer is anodically bonded to Pyrex and finally diced into individual devices. This has been a standard technique for fabricating silicon pressure sensors and micropumps for many years.

Recently, however, *surface micromachining*, *silicon fusion bonding*, and a process called *LIGA* (Lithographie, Galvanoformung, Abformung) have also emerged as major fabrication techniques. Surface micromachining of a wafer involves selectively applying or removing thin film layers. Thin film deposition and wet and dry etching techniques are the primary tools for this. Thin films of polysilicon, silicon oxide, and silicon nitride are used to produce sensing elements, electrical interconnections, and the structural, mask, and sacrificial layers. Silicon epitaxial layers, grown and deposited silicon oxide layers and photoresist are used as sacrificial materials.

A typical surface micromachining process is depicted in Figure 8.<sup>6</sup> A sacrificial layer is applied (grown or deposited) in an appropriate pattern on the wafer and then removed from the areas where a mechanical structure will be attached to the substrate. Then, the mechanical layer is applied and patterned. Finally, the underlying sacrificial layer is etched away to release the mechanical structure. This process can produce structures on a scale of a few hundred micrometers, such as the microgripper appearing in Figure 9. This microgripper was fabricated by Berkeley Sensor and Actuator Center, CA using released-polysilicon surface micromachining and is activated by electrostatic forces.<sup>6</sup>

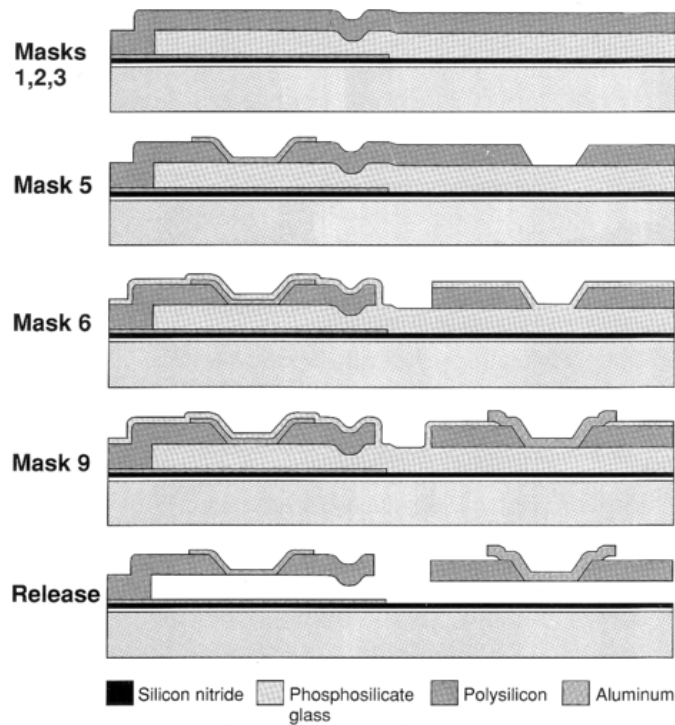


**Figure 8** A typical surface micromachining process. The phosphosilicate glass layer is sacrificial in this process.<sup>6</sup>

The first step of the LIGA process involves generating a photoresist pattern on a conductive substrate using deep x-ray lithography. The gaps between the resist patterns can be fully electroplated, yielding a highly accurate negative replica of the original resist pattern. This can be used as a mold for plastic resins such as polyimide and polymethyl methacrylate or for ceramic slurries. Once the material has been cured, the mold is removed, leaving behind microreplicas of the original pattern. An epicyclic microgearbox appears in Figure 10 that is to be fitted onto the micromotor pictured in Figure 6. It contains seventeen microinjection-molded components made from the polymer POM.<sup>5</sup> Note that the chief disadvantage of this process is the need for a short-wavelength, highly collimated x-ray source, ideally a synchrotron. Few MEMS manufacturers can afford their own synchrotron.

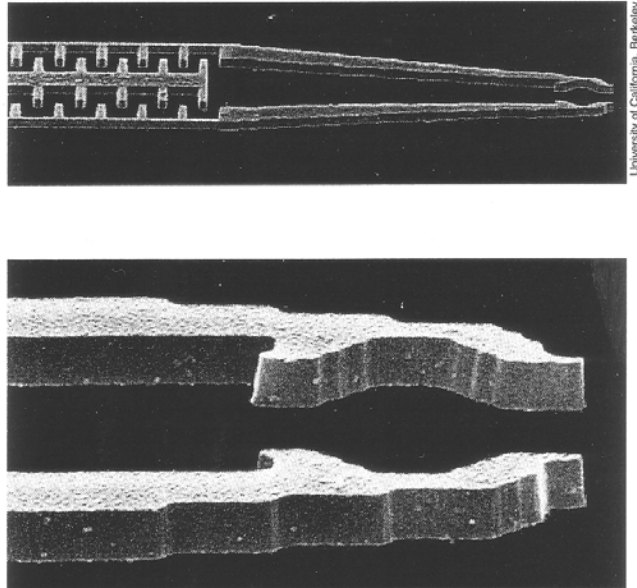


**Figure 9** A microgripper fabricated by Berkeley Sensor and Actuator Center, CA using released-polysilicon surface micromachining.<sup>6</sup>

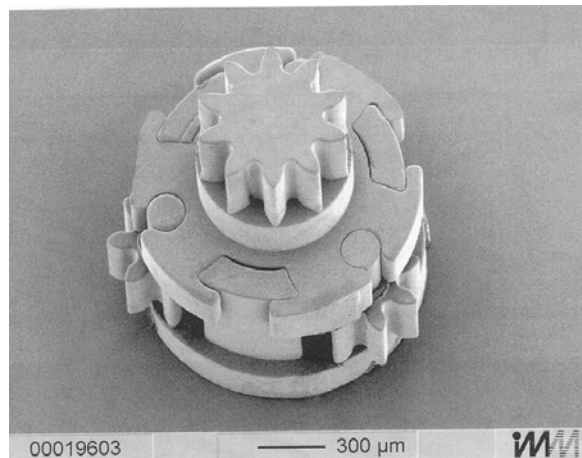


**Figure 10** A microgearbox made of polymer POM using a LIGA technique. It will be fitted onto the micromotor pictured in Figure 6.<sup>5</sup>

#### (4) Artificial Muscle

In a manner similar to the silicon MEMS devices, the operation of polymer film actuators is based on electrostatic principles. The artificial muscle described here, developed at the University of Tokyo, makes use of this type of actuator.<sup>7</sup>

The basic design and operation of the polymer film actuator is depicted in Figure 11. Two polymer films with embedded electrodes are placed adjacent to each other. When three-phase voltages (+V, -V, 0) are applied in succession to every three embedded electrodes in the stator film [Figure 11a], charges of -Q, +Q and 0 are induced

on the opposing slider film [Figure 11b]. Then, when the three voltages are switched to  $-V$ ,  $+V$  and  $-V$  [Figure 11c], a repulsive force is generated between the stator and slider films, and an attractive force is generated between the adjacent electrodes on the two films. This produces an electrode pitch displacement (in this case a shift of the slider to the right) [Figure 11d]. The electrostatic force generated increases significantly as the electrode gap is reduced.

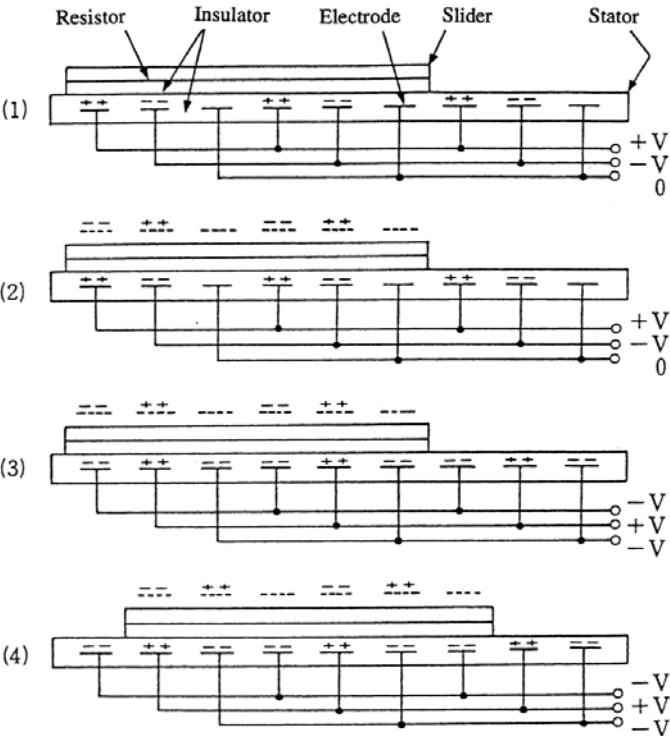


**Figure 11** The basic design and operation of a polymer film actuator.<sup>7</sup>

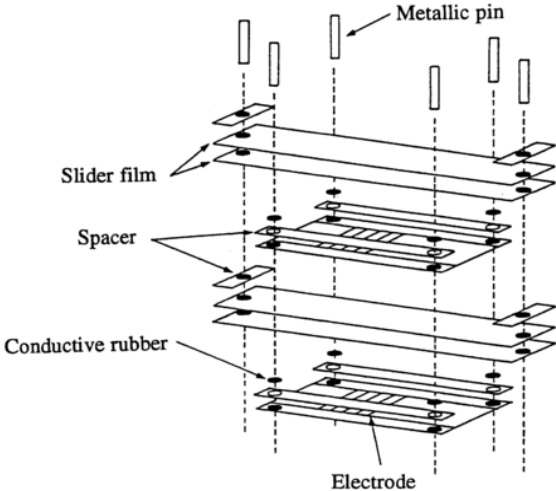


**Figure 12** Construction of the electrostatic polymer artificial muscle.<sup>7</sup>

The construction of the electrostatic polymer artificial muscle is illustrated in Figure 12. A thin film of PET, 12  $\mu\text{m}$  in thickness, is used for the slider, to which a polyimide film with surface line electrodes is laminated which serves as the stator. Spacers are included in the structure as shown to maintain the proper separation between electroded surfaces. Five stator/slider pairs, 34 mm in width and 80 mm in length, are stacked together with a 0.35 mm gap between them. The prototype structure, which weighs 43 g is then dipped into “Fluorinat (3M).” When three-phase voltage at 10 Hz is applied with a pitch range of 0.1–1.0 mm, a speed of 1 m/sec is achieved without load. A propulsive force (thrust) of 1–3 N is possible with an applied root-mean-square voltage of 2.5 kV. The relatively high voltage required for operation is a major drawback of this artificial muscle.

A robot arm driven by the electrostatic artificial muscles is shown in Figure 13. A 40-layer electrostatic actuator (generating 320 N) works in conjunction with a 20-layer actuator (generating 160 N) via a pulley mechanism.<sup>8</sup>

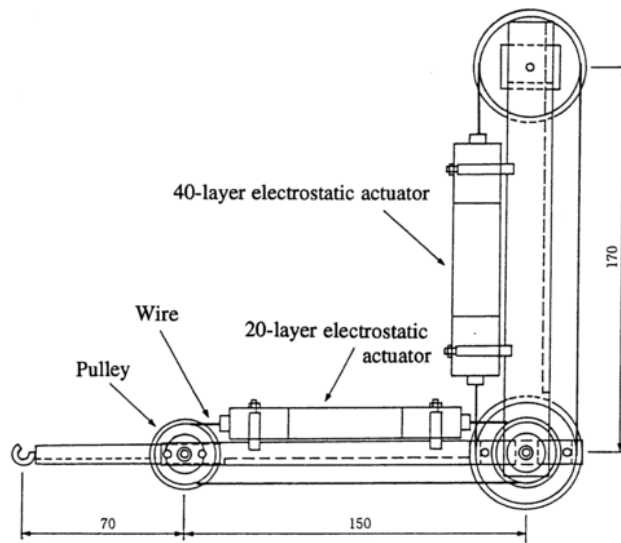


**Figure 13** Schematic representation of a robot arm incorporating two artificial muscles.<sup>8</sup>

## (5) Shape Memory Alloys

Many materials exhibit large mechanical deformations when undergoing a structural phase transition. This phase transition may be induced by temperature, stress, or electric field. In some materials, once the mechanical deformation is induced, some deformation may be retained with the release of the load and applied stress, but the original form may be restored with the application of heat. This type of action is called *shape memory*.

The stress versus strain curves for typical shape memory and super-elastic alloys and a normal metal are shown in Figure 14.<sup>9</sup> When the stress applied to a normal metal exceeds the elastic limit, irreversible (non-recoverable) plastic deformation results. A super-elastic alloy subjected to the same level of stress, on the other hand, will become elastically soft at a level beyond the elastic deformation limit, due to a stress-induced phase transformation. The deformation that occurs in this case, however, is reversible and the original form is recovered as the load is removed and the stress is released. Finally, we see in the case of the shape memory alloy, a response quite similar to the normal metal except that for these materials the original form may be recovered after the load has been removed by heating the alloy at the appropriate temperature.

Depending on the temperature at which it is deformed, a shape memory alloy may exhibit one of two different types of mechanical behavior: *superelastic* or *pseudoplastic*. When Nitinol (a Ni-Ti alloy) is behaving as a *superelastic* material, reversible deformation of up to 10% may be obtained with a very small effective modulus, which is

several orders of magnitude smaller than the modulus of the parent phase. When the material is *pseudoplastic*, the deformation occurs with some slight hardening accompanied by very large strains. The pseudoplastically deformed alloy can then be restored to its initial shape by heating. The generative force may be as high as  $10^8 \text{ N/m}^2$  during the recovery process.

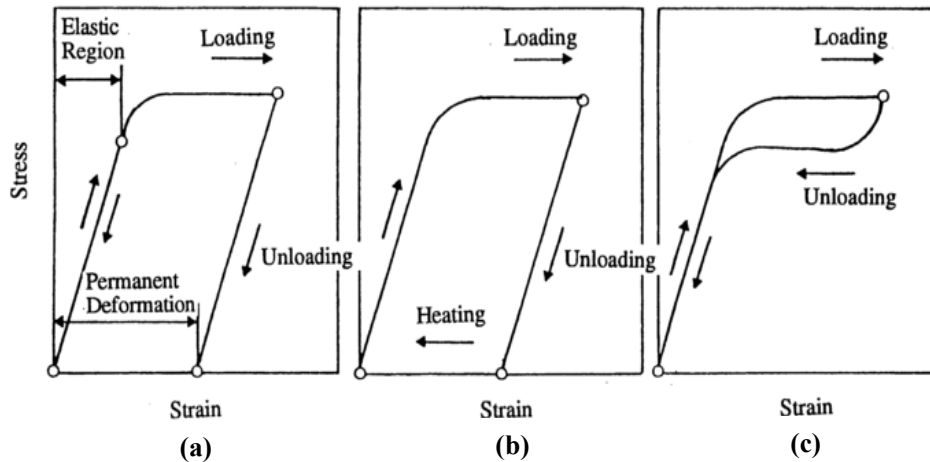


**Figure 14** Typical stress versus strain curves for: (a) normal, (b) shape memory, and (c) super-elastic materials.<sup>9</sup>

The *shape memory* and *superelastic* mechanisms are considered from a crystallographic viewpoint in Figure 15.<sup>10</sup> In a normal metal, atomic shifts occur above a certain critical stress, leading to a shear strain, which remains as a permanent residual strain even after the stress is removed [Figure 15(a)]. In a shape memory alloy, a *Martensitic phase transformation* occurs under these conditions; if the parent phase (Austenite) is below the transition temperature, the Martensite phase will be induced. Macroscopically the material will retain the same shape, but on a microscopic level many twin structures will have been generated. Since the twin planes are easily moved, the Martensite material is readily deformed by the external stress [Figure 15(b)]. However, when the deformed material is heated to a temperature higher than the reverse phase transition temperature,  $A_f$ , the parent phase (*Austenite*) is induced and the initial shape is recovered. This is the *shape memory effect*. If stress is applied to a shape memory alloy above the transition temperature,  $A_f$  (that is, in the Austenite phase), above a certain stress level the Martensite phase is induced gradually, leading to a pseudo-plastic response. The material is very compliant under these conditions. As the applied stress is decreased, the reverse phase transformation (Martensite to Austenite) occurs and the material returns to its original elastically stiff state. This elastic phenomenon, which is similar to what is observed for rubber, is called *superelasticity*.

Interestingly, one of the first commercial successes involving the shape memory alloy was in women's lingerie. One brassiere design incorporating the alloy exploited the material's superelastic properties to help maintain a comfortable fit while providing adequate support. Another big market has been for pipe couplers and electrical connectors.<sup>11</sup> The couplings are made by machining a cylinder of the alloy while it is in the Austenite phase, usually with circumferential sealing bands on the inner diameter. A second, slightly wider cylinder is then inserted into the shape memory cylinder as it cools in order to force it to expand as the material transforms to the Martensite phase. When the coupling is brought back to room temperature, the outer cylinder contracts as it reverts to the Austenite phase, tightly clamping the inner cylinder.

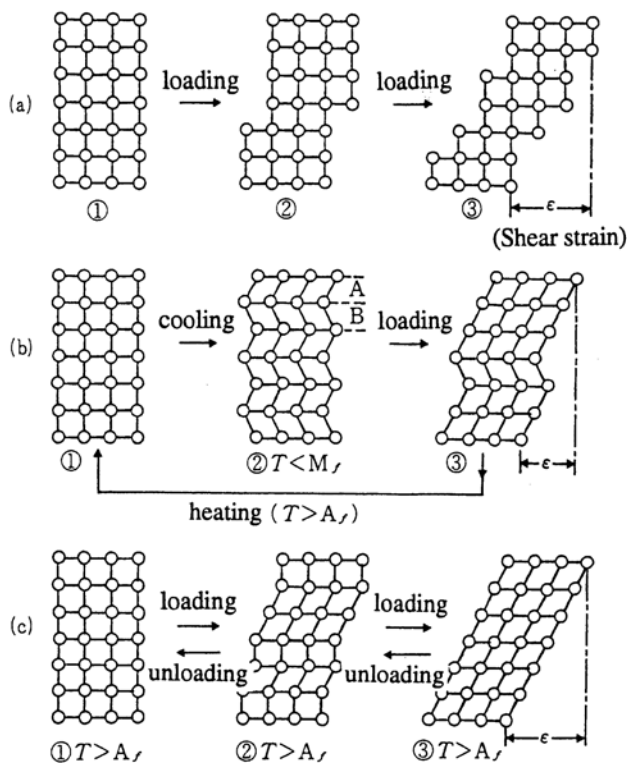


**Figure 15** Microscopic lattice distortions for: (a) normal, (b) shape memory, and (c) super-elastic metals.<sup>10</sup>

An actuator incorporating a shape memory spring is shown in Figure 16. A normal steel spring and a shape memory alloy (Ni-Ti or Nitinol) spring, which will “remember” its fully extended form, are included in the design. At low operating temperatures, the shaft will be pushed to the right as the shape memory spring becomes soft. When the temperature is raised (for example, by means of an electric current), the spring constant of the shape memory actuator will increase significantly, causing the shaft to be pushed to the left.

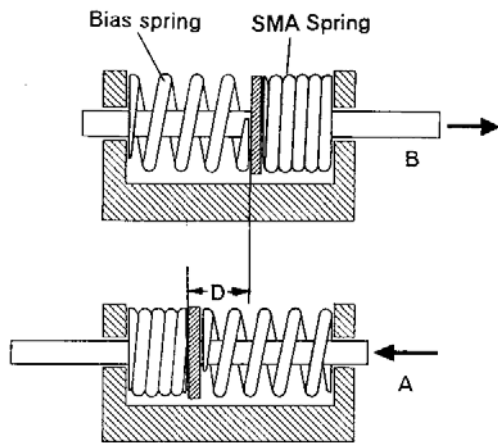


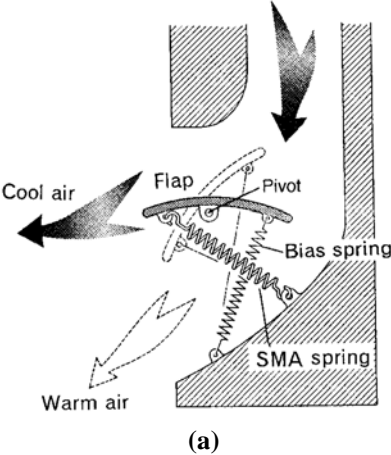
**Figure 16** A two-way actuator incorporating shape memory alloy (SMA) and normal metal (Bias) springs.

A similar mechanism is utilized in the flapper control unit for an air conditioning system. The temperature of the air passing from the air conditioner is constantly changing and can sometimes become uncomfortably cold. One solution to this problem is to adjust the air flow direction using a flap mounted on the front of the air conditioner that is actuated by a shape memory alloy as shown in Figure 17.<sup>12</sup> When the flowing air is cold, the flap will move so as to direct the air upward, and when the air temperature exceeds body temperature, it will move so as to direct the air downward. The link mechanism and the rocking motion of the flap are illustrated in Figure 17(a). The shape memory spring and bias spring act on the ends of the flapper to swing it like a seesaw about the pivot, thus redirecting the air flow as the temperature changes.

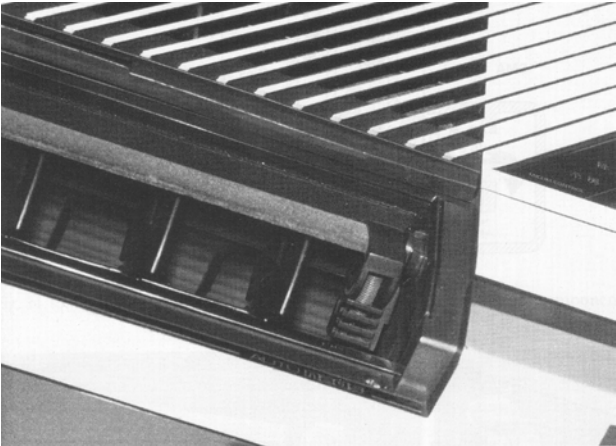
**(6) Magnetostrictive Actuators**

Magnetostrictive materials convert magnetic energy into mechanical energy and vice versa. A magnetostrictive material becomes strained when it is magnetized. Conversely, when either an applied force or torque produces a strain in a magnetostrictive material, the material’s magnetic state (magnetization and permeability) will change.

Magnetostriction is an inherent material property that depends on electron spin, the orientation and interaction of spin orbitals, and the molecular lattice configuration. It is also affected by domain wall motion and rotation of the magnetization under the influence of an applied magnetic field or stress.<sup>13</sup>



(a)



(b)

**Figure 17** An air conditioning system with a shape memory flapper control mechanism: (a) schematic representation of the flapper control mechanism and (b) the flapper control unit as it appears in an actual air conditioner.<sup>12</sup>

Research on giant magnetostriction began with studies on Terfenol-D (a Tb-Dy-Fe alloy) conducted by Clark et al.<sup>14</sup> Longitudinally and transversely induced strain curves at various temperatures for Terfenol-D appear in Figure 18. The domain wall motion induced with the application of a small magnetic field occurs due to the growth of domains having magnetization aligned with the applied field, at the expense of domains with magnetization opposing the field. At moderate field strengths, the magnetic moments within unfavorably oriented domains overcome the anisotropy energy and suddenly rotate such that one of their crystallographic easy axes is more closely aligned with the external field direction. This sudden rotation is generally accompanied by a large change in strain. As the field is increased further, the magnetic moments undergo coherent rotation until they are completely aligned with the applied field. At this point the material is single-domain and the strain curve becomes saturated.

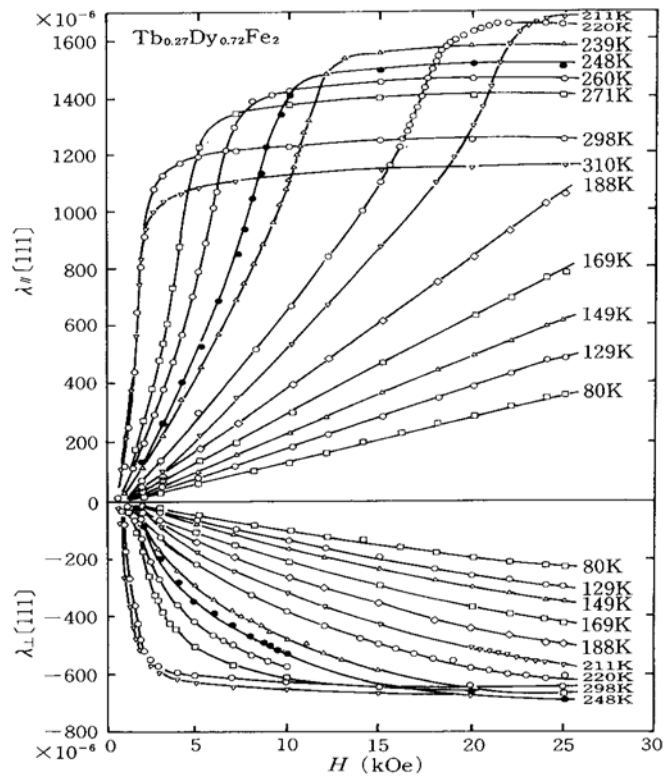


**Figure 18** Longitudinally and transversely induced strains in Terfenol-D at various temperatures.<sup>14</sup>

Although one can attain strains exceeding 0.17 % and sufficiently large generative stresses with magnetostrictive materials of this type, problems similar to those encountered with electromagnetic motors arise. These are related to the need for a magnetic coil and high field strengths to drive the devices. A typical design for a giant magnetostrictive actuator is depicted in Figure 19.<sup>15</sup> Two noteworthy features of this actuator are the pre-stressing mechanism and the magnetic coil and shield, which significantly increase the overall volume and weight of the system. The extensional pre-stress is important for optimum performance of the magnetostrictive alloy, and in some cases, a bias magnetic field must be maintained because the induced strain tends to be rather insensitive to the external field at low field strengths.

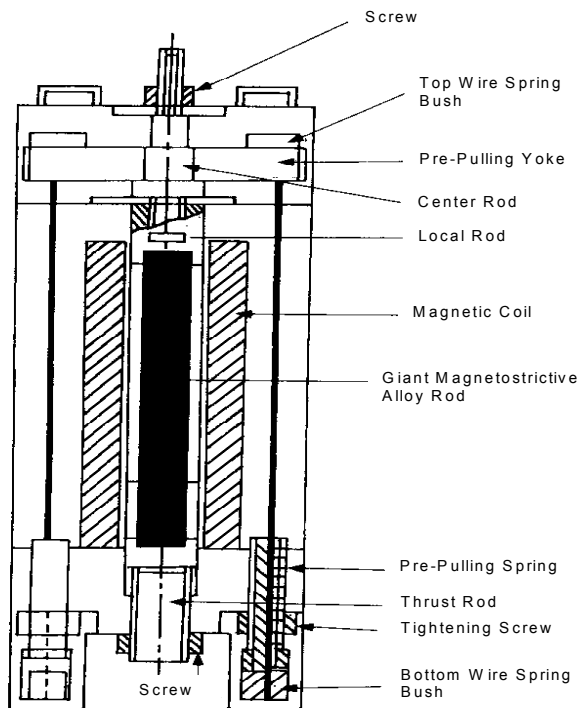


**Figure 19** A typical design for a giant magnetostrictive actuator.<sup>15</sup>

The sonar device depicted in Figure 20 includes a square array of four magnetostrictive (Terfenol-D) rods mounted in a metal ring.<sup>16</sup> The magnetostrictive rods are 6 mm in diameter and 50 mm in length, and have a free resonance frequency of 7.4 kHz. The resonance frequency of the entire ring device is 2.0 kHz.

In general, magnetostrictive actuators such as these are bulky due to the magnetic coil and shield required for their operation, and, hence, are difficult to miniaturize. On the other hand, since they can generate relatively large forces and their efficiency increases with increasing size, they tend to be especially suitable for applications often reserved for electromagnetic motors, such as in construction/demolition machines and for vibration control in large structures. Another intriguing application can be found in surgery, where miniature magnetostrictive actuators, controlled with external magnetic fields provided by means of technology similar to what is currently used in MRI machines, can be used for specialized procedures.

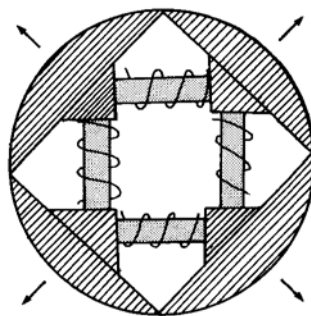


**Figure 20** A high power acoustic transducer incorporating four magneto-strictive actuators.<sup>16</sup>

## (7) Piezoelectric/Electrostrictive Actuators

When an electric field is applied to an insulating material, strain will be induced in the material either through the piezoelectric effect, electrostriction, or a combination of the two effects. The *converse piezoelectric effect* is a primary electromechanical effect, where the induced strain is proportional to the applied electric field, while the electrostrictive effect is a secondary phenomenon, whereby the induced strain is proportional to the square of the applied field. A brief introduction to this class of devices is given here. A more thorough description of the piezoelectric effect and electrostriction will be presented in the next chapter.

Electric field-induced strain curves are shown for piezoelectric lanthanum-doped lead zirconate titanate (PLZT) and electrostrictive lead magnesium niobate (PMN)-based ceramics in Figure 21.<sup>17</sup> The piezoelectric response shows the characteristic linear strain versus field relation with a noticeable hysteresis, while the electrostrictive response exhibits no hysteresis and a non-linear relation between the induced strain and the applied electric field is apparent. Due to this non-linear behavior, a sophisticated drive circuit is generally needed for electrostrictive actuators. Note that the maximum strain and stress levels for the piezoelectric ceramics are around 0.1 % and  $4 \times 10^7 \text{ N/m}^2$ , respectively.

Among all the solid-state varieties, piezoelectric actuators have undergone the most advanced development and remain the most commonly employed type for many applications at this time. The dot matrix printer head pictured in Figure 22, which operates by means of a multilayer piezoelectric actuator with sophisticated displacement amplification mechanisms, is one earlier application that was commercialized by NEC of Japan in 1987.<sup>18</sup>

Piezoelectric ultrasonic motors have also been developed intensively. Electronic component industries have currently focused their attention on the development of these devices, mainly because the piezoelectric motors offer distinct advantages of superior efficiency, miniature size (5-8 mm), and ease of manufacturing over conventional electromagnetic motors. Microultrasonic motors developed and commercialized by SEIKO Instruments, Japan for wristwatch applications appear in Figure 23.<sup>19</sup> The 8 mm diameter motor is used as a silent alarm, and the 4 mm diameter motor is part of a date change mechanism.

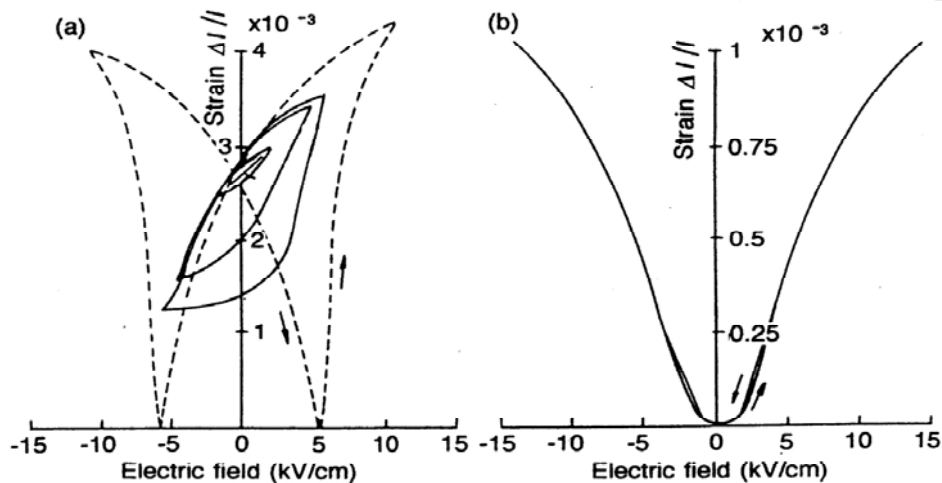


**Figure 21** Electric field-induced strains in (a) piezoelectric lanthanum-doped lead zirconate titanate, and (b) electrostrictive lead magnesium niobate-based ceramics.<sup>17</sup>

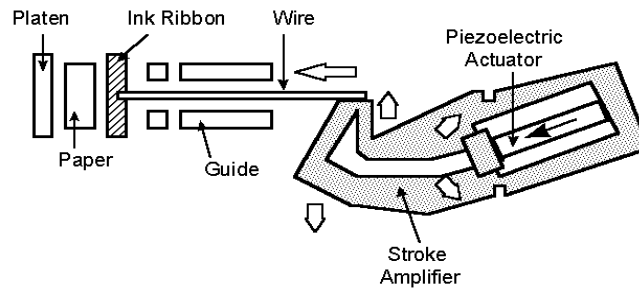


**Figure 22** A dot matrix printer head incorporating a multilayer piezoelectric actuator and a hinge-lever type displacement amplification mechanism (NEC, Japan).<sup>18</sup>



**Figure 23** Micro-ultrasonic motors utilized for silent alarm (8 mm diameter, left-side) and date change (4 mm diameter, right-side) mechanisms in a wristwatch (SEIKO, Japan).<sup>19</sup>

### (8) Polymer/Elastomer Actuators

Large strains can be generated in polymer materials without causing mechanical damage because of their high elastic compliance. Polymer actuator materials can be classified according to two general types: *polyvinylidene difluoride (PVDF)-based piezoelectric polymers* and *electret/elastomer* types.

Copolymers from the system polyvinylidene difluoride trifluoroethylene [P(VDF-TrFE)] are well-known as piezoelectric materials. The strain induced in these materials is not very large, however, due to the very high coercive field. An electron irradiation treatment has been applied to materials from this system by Zhang et al. which significantly enhances the magnitude of the induced strain.<sup>20</sup> A 68/32 mole percent P(VDF-TrFE) copolymer film is irradiated by a 1.0 MeV electron beam at 105°C. The 70 Mrad exposure results in a diffuse phase transition and a decrease in the transition temperature as compared with the non-irradiated material. It is believed that the observed changes in the phase transition are due to the development of a microdomain state, similar to that associated with relaxor ferroelectrics, which effectively interrupts the long-range coupling of ferroelectric domains. The strain curve pictured in Figure 24 for an irradiated P(VDF-TrFE) specimen demonstrates that induced strains as high as 5% are possible with an applied field strength of 150 MV/m.

Elastomer actuators operate through the *Maxwell force* that occurs in an electrostatic capacitor. Considering a capacitor with an area,  $S$ , and electrode gap,  $t$ , filled with a dielectric material with a dielectric constant,  $K$ , the capacitance,  $C$ , and the stored energy,  $U$ , will be given by:

$$C = \epsilon_0 K (S/t), \tag{1}$$

$$U = (1/2)CV^2 \tag{2}$$

Note that an attractive force described by

$$F = (\partial U / \partial t) = - (1/2) \epsilon_0 K S (V/t)^2 \quad (3)$$

will be induced between the electrodes, which will lead to a decrease in the inter-electrode distance. Hence, we see that a larger displacement can be obtained by increasing the elastic compliance and the effective permittivity (and, therefore, the stored electric charge) of the material. A hybrid elastomer structure has been developed whereby a porous PTFE and a stiff PFCB phase are incorporated in the configuration depicted in Figure 25.<sup>21</sup> The stiffer PFCB phase serves to store the charge while the porous PTFE phase effectively increases the overall compliance of the structure. An effective piezoelectric  $d_{33}$  strain coefficient of around 600 pC/N, has been obtained for this composite structure, which is 20 times larger than that obtained for pure PVDF. In theory, one can reasonably predict a strain level as high as 100% (a twofold enhancement) for this material when a sufficiently soft polymer is used as the porous phase. It is important to note that even though one might feasibly anticipate large displacements for a polymer, they will be realized only at the expense of the generative force and responsivity of the device.

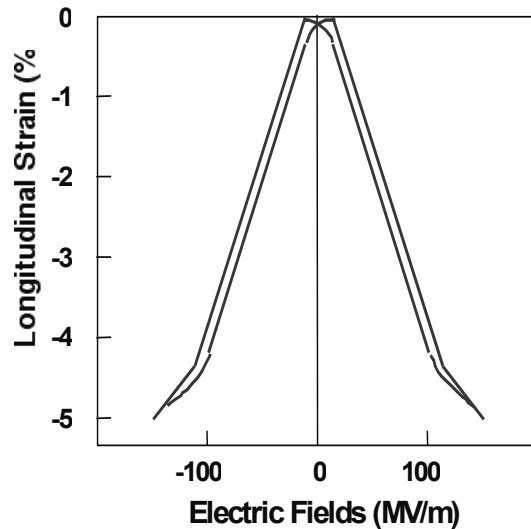


**Figure 24** The electric field-induced strain curve for an irradiated polyvinylidene difluoride-based copolymer.<sup>21</sup>

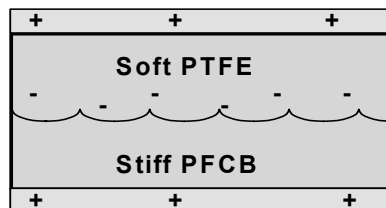


**Figure 25** Schematic representation of a hybrid elastomer structure incorporating a porous PTFE and a stiff PFCB phase.<sup>21</sup>

## (9) Photostriction

The ongoing emphasis on miniaturization and the integration of microrobotics and microelectronics has resulted in significant development of new ceramic actuators. Those utilizing wavelength-dependent optical actuation mechanisms are especially attractive at this time. *Photostrictive actuators*, which convert the photonic energy into mechanical motion, are of interest for their potential use in microactuation and microsensing applications. Optical actuators are also attractive for use as the driving component in optically controlled electromagnetic noise-free systems. The photostrictive effect has also been used recently for a photophonic device, in which light is transformed into sound through the mechanical vibration induced by intermittent illumination.

In principle, the *photostrictive effect* arises from a superposition of the photovoltaic effect (the generation of a potential difference in response to illumination), and the converse piezoelectric effect (strain induce by an applied electric field).<sup>22</sup> The photostrictive effect has been studied mainly in ferroelectric polycrystalline materials. Lanthanum-modified lead zirconate titanate (PLZT) ceramic is one of the most promising photostrictive materials due to its relatively high piezoelectric coefficient and ease of fabrication. The origin of the photovoltaic effect in (PLZT) is not yet clear, although several models for possible mechanisms have been proposed. Key issues in understanding the mechanisms behind the effect are both impurity doping and crystal asymmetry. One model has been proposed that describes the effect in terms of the electron energy band structure for PLZT ceramics.<sup>23</sup> According to this model, the donor impurity level associated with the lanthanum doping will occur slightly above the valence band as depicted in Figure 26. The asymmetric potential due to crystallographic anisotropy is expected to facilitate the transition of the electron between these levels by providing it with *preferred momentum*. An asymmetric crystal exhibiting a photovoltaic response should also be piezoelectric and, therefore, a photostrictive response is also expected through the coupling of the two effects.

Application of the photostriction effect has been demonstrated with the PLZT ceramic photo-driven relay and microwalking devices developed by Uchino et al.<sup>24</sup> These devices are activated entirely by the incident light and require no drive circuitry.

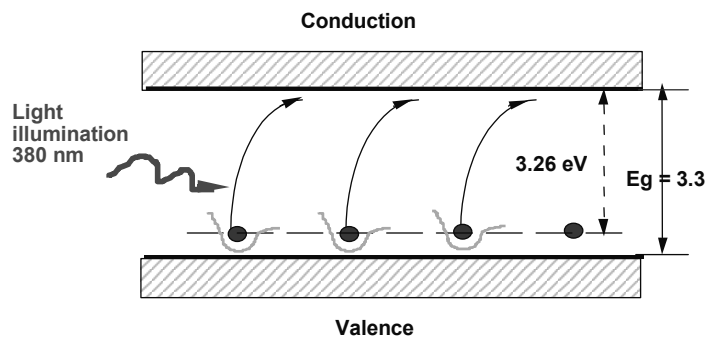


**Figure 26** A current source model for the photovoltaic effect in PLZT.<sup>23</sup>

Recently, a new application for highly efficient photostrictive PLZT films on flexible substrates has been proposed for use in a new class of small exploratory land vehicles for future space missions.<sup>25</sup> The original  $\pi$ -shaped design of the micro-walking device can be modified to assume the arch shape pictured in Figure 27. It is comprised of a photoactuating composite film, similar to that conventionally used for unimorphs, fabricated in the form of an arch on which the triangular top piece is attached. The device executes the motion depicted in the figure when illuminated. Optimum photostrictive response has been observed for devices incorporating PLZT films approximately 30  $\mu\text{m}$  in thickness. The device is driven at resonance with chopped illumination. Photomechanical resonance has been demonstrated in a PLZT bimorph.<sup>26</sup> Photoactuating films have been produced from PLZT solutions and applied to one side of a suitable flexible substrate designed to assume a curvature of 1  $\text{cm}^{-1}$ . The walking device is designed to have a small difference in length between the right and left legs in order to establish a slight difference between their resonance frequencies. A chopped light source operating near these resonance

frequencies is used to illuminate the device in order to induce the optimum vibration of the bimorph. Rotation of the walker in either the clockwise or counterclockwise directions is achieved by tuning the source to match the resonance frequency of one or the other leg.

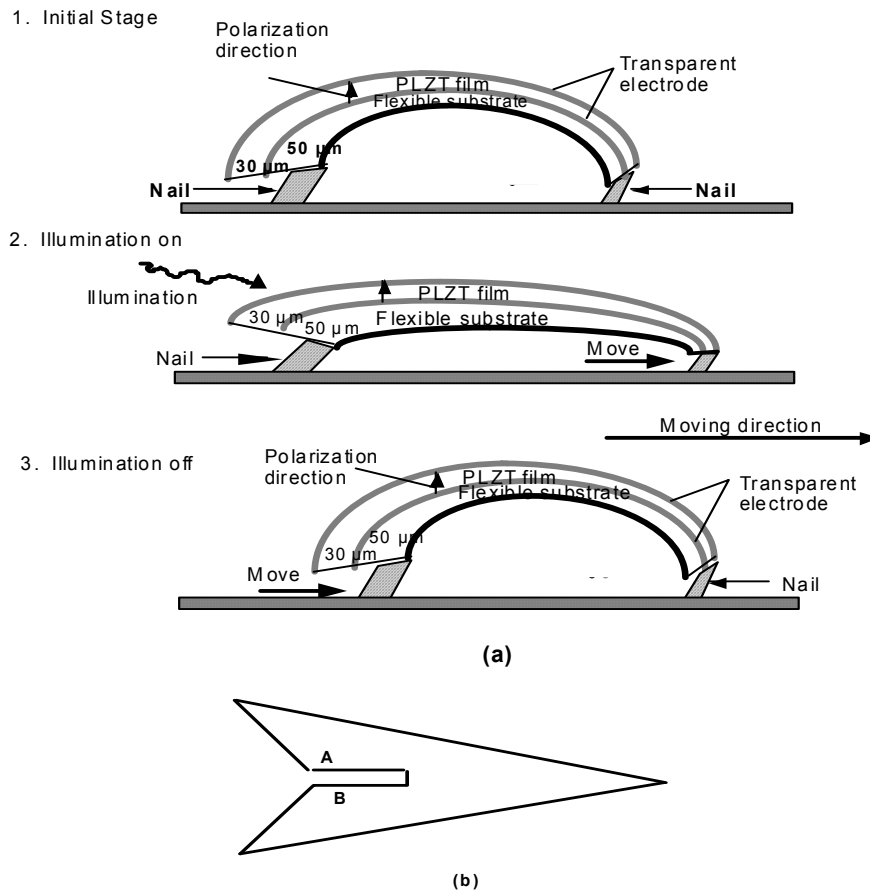


**Figure 27** Schematic representation of an arch-shaped photoactuating film device: (a) action sequence and (b) the triangular top piece.<sup>25</sup>

### (10) Electro/magnetorheological Fluids

Composite materials whose rheological properties can be changed with the application of an electric or a magnetic field are referred to as *electrorheological* (ER) or *magnetorheological* (MR) materials, respectively. The ER and MR materials are generally in the liquid state. The rheological state of such fluids is affected when dipoles are induced in the suspension by the applied field. The dipoles interact to form columnar structures parallel to the applied field as depicted in Figure 28. These chain-like structures restrict the flow of the fluid, thereby increasing the viscosity of the suspension.

Electrorheological (ER) fluids are composed of electrically polarizable particles suspended in an insulating medium. Ferroelectric particles, such as barium titanate and strontium titanate, are typically used in ER fluids because they have relatively high dielectric constants. On the other hand, magnetorheological (MR) fluids have a high concentration of magnetizable particles in a nonmagnetic medium. Spherical iron particles obtained from the thermal decomposition of iron pentacarbonyl are commonly used.<sup>27</sup>

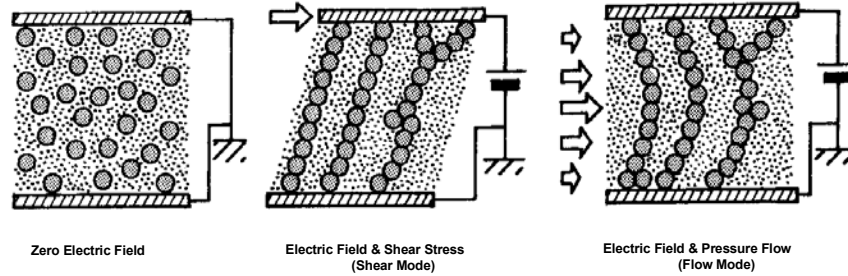


**Figure 28** Schematic representation of the response of an electrorheological fluid to applied electric field and stress.

The properties of typical ER and MR fluids are summarized in Table 4. In general, ER and MR fluids are almost identical in terms of their rheological characteristics. However, from a production point of view, the MR fluid is preferred over the ER variety, because its properties are less affected by impurities.

**Table 4** Properties of typical ER and MR fluids.

Property	ER Fluid	MR Fluid
Maximum Yield Strength	2-5 (kPa)	50-100 (kPa)
Maximum Field	4 (kV/mm)	250 (kN/Am)
Plastic Viscosity	0.1-1.0 (Pa-s)	0.1-1.0 (Pa-s)
Temperature Range	+10-90 (°C) [dc] -10-125 (°C) [ac]	-40-150 (°C)
Response Time	msec	msec
Density	1-2 (g/cm <sup>3</sup> )	3-4 (g/cm <sup>3</sup> )
Maximum Energy Density	0.001 (J/cm <sup>3</sup> )	0.1 (J/cm <sup>3</sup> )
Typical Power Supply	2-5 (kV)/1-10 (mA)	2-25 (kV)/1-2 (mA)
Impurity Sensitivity	intolerant	unaffected

The yield stress and apparent viscosity of the fluids increase with the applied field because the mechanical energy required to induce and to maintain these chain-like structures increases with increasing field strength. The storage modulus is plotted as a function of applied electric field for silicone elastomers containing 20-30% iron in Figure 29.<sup>28</sup> These elastomers exhibit significant variations in modulus with increasing electric field. The shear storage modulus was also found to be dependent on the alignment of the particles in the elastomer.

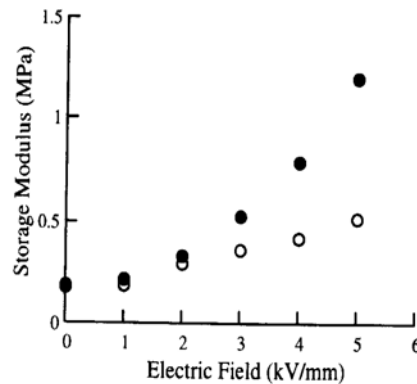


**Figure 29** The storage modulus plotted as a function of applied electric field for silicone elastomers containing 20-30% iron.<sup>28</sup> [Random (o) and Aligned (●) particle orientation states]

The basic modes of operation for ER and MR fluids are illustrated in Figure 30. Magnetorheological fluid foam dampers are effective and exhibit long life. Little wear of the foam matrix occurs as the stresses are carried by the field-induced chain structure of iron particles in the MR fluid. A caliper type MR fluid brake design is depicted in Figure 31. Rather than a fully enclosed housing, the absorbent foam filled with MR fluid is attached to the pole faces of the steel yoke. These magnetorheological fluid-based devices have been successfully commercialized for use in exercise equipment<sup>29</sup> and in vehicle seat vibration control.<sup>30</sup>

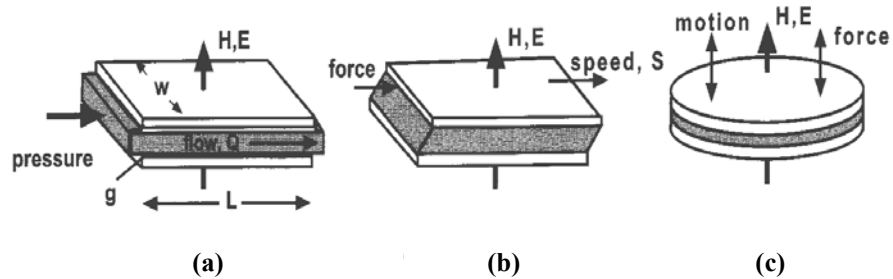


**Figure 30** Basic modes of operation for ER and MR fluids: (a) valve mode, (b) direct shear mode, and (c) squeeze mode.

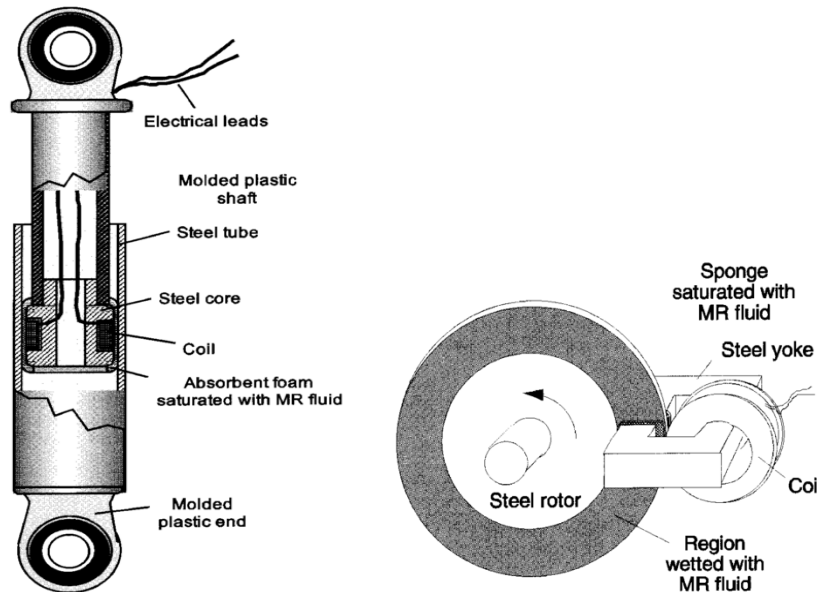


**Figure 31** Construction of two simple, low cost magnetorheological (MR) foam devices: (a) a vibration damper<sup>30</sup> and (b) a rotary caliper brake<sup>29</sup>. (Lord Corp.)

### (11) Comparison among the Solid-State Actuators

The specifications for shape memory, magnetostrictive, piezoelectric and electrostrictive actuators are listed in Table 5. Certain characteristic features of each type become evident upon examining these data. The *shape memory actuators*, which operate in response to a temperature change, require a relatively large amount of input energy and typically have rather slow response speeds. A flat strip of Ni-Ti alloy, which alternates in form between an arc shape and an unbent strip to transfer energy to a spring, however, can be deformed repeatedly by heating and cooling via an electric current.

The magnetostrictive actuator likewise demonstrates some advantages and disadvantages. Although some magnetic alloys (such as Terfenol-D) may exhibit relatively large induced strains, more commonly, the strain induced in this class of actuator is small. An additional drawback to this variety is the need for a driving coil, which in many applications can be troublesome; Joule heating is inevitable, and magnetic field leakage prevents it from being used adjacent to an operational amplifier or some other type of integrated circuit.

On the other hand, piezoelectric strain and electrostriction is induced by an electric field, and relatively large strains can be obtained in a variety of materials. Hence, the *piezoelectric* and *electrostrictive actuators* are considered the most promising. Lead zirconate titanate (PZT)-based piezoelectric ceramics are most commonly used due to their availability, linear characteristics, low driving energy (low permittivity), and temperature stability at room temperature, as compared to the electrostrictive devices. Electrostrictive actuators are preferred for applications where there may be significant temperature variations (such as experienced by components used on the space shuttle) or high stress conditions (as occur for cutting machine devices). In terms of their reliability, electrostrictive materials are considered better than piezoelectrics in these cases, because they exhibit significantly less degradation and aging under severe conditions.

**Table 5** Specifications for shape memory, magnetostrictive, piezoelectric and electrostrictive actuators.

	Shape Memory	Magnetostrictive	Piezoelectric	Electrostrictive
Strain ( $\Delta l/l$ )	$10^{-3}$ - $10^{-2}$	$10^{-4}$ - $10^{-3}$	$10^{-3}$ - $10^{-2}$	$10^{-4}$ - $10^{-3}$
Hysteresis	Large	Large	Large	Small
Aging	Large	Small	Large	Small
Response	sec	$\mu$ sec	msec	$\mu$ sec
Drive Source	Heat	Magnetic Coil	Electric Field	Electric Field

## 4. CRITICAL DESIGN CONCEPTS

### (1) Design Concepts Involving Smart Actuators

The performance of smart actuators is dependent on complex factors, which can be divided into three major categories: (1) the material properties, (2) the device design, and (3) the drive technique. The devices and systems to be presented in the following chapters will be described and characterized in terms of these primary factors.

In order to illustrate the significance of these factors with regard to the design of a device or system, let us focus for the moment just on piezoelectric devices. One material-related concern of primary importance will be the optimization of the piezoceramic or single crystal composition, which may involve the incorporation of dopants. The orientation of a single crystal material is also of importance. Control of material parameters such as these are necessary in order to optimize the strains induced under high stroke level drive and to stabilize temperature and external stress dependences. The design determines to a large extent the performance, durability, and lifetime of the device. The inclusion of some failure detection or "health" monitoring mechanism in the actuator is expected to increase its reliability significantly. When considering drive techniques, the pulse drive and ac drive modes require special attention. The vibration overshoot that occurs after applying an abrupt leading edge step/pulse voltage to the actuator will cause a large tensile force and a sustained applied AC voltage will generate considerable heat within the device. The product of such a design will be one for which all of these parameters have been optimized.

### (2) Future Trends of Smart Actuators

Much of the current interest in ceramic actuators stems from the development of smart materials and structures. The evolution of this family of materials is gradually progressing through stages ranging from trivial functionality to *smart* to *intelligent* and finally to a more "wise" mode of operation. As already discussed, the off-diagonal couplings listed in Table 2 all have corresponding converse effects (such as, the piezoelectric and converse-piezoelectric effects) so that both "sensing" and "actuating" functions can be realized in the same materials. One example of such a material is that employed in the electronic modulated automobile shock absorber developed by

Toyota Motors, which is pictured in Figure 32.<sup>31</sup> The sensor used to detect the road roughness and the actuator used to modify the valve position to change the shock absorbing rate are both multilayer piezoelectric devices. The soft absorbing mode of operation provides the comfortable ride one expects in a vehicle such as a luxury limousine, while the hard absorbing mode provides the good steering control one might desire in a truck or sport utility vehicle. This smart suspension system can also provide both controllability and comfort simultaneously, depending on road conditions.

Mohandas Gandhi, a famous Indian leader, compiled the “The Seven Blunders of the World,” in which we find very important principles that also apply in developing new devices. “Science without Humanity” is one of them. We have referred to the fact that in the future we may need to incorporate fail-safe mechanisms or some other “wise” function in our devices or systems to determine whether “this response may cause harm to humans” or “this action will lead to environmental destruction,” and to respond accordingly.

In addition to the fail-safe mechanisms referred to earlier in this chapter, we can consider this idea of a “wise” system in a somewhat broader sense. Not long ago, the author met an enthusiastic, middle-aged researcher in Tokyo. He was working on a piezoelectric actuator system for artificial insemination and proudly declared that their system could impregnate cows precisely and quickly, at the rate of some two hundred per hour. One question that might come to mind in considering such a system is: What are the moral/ethical implications of this sort of mass production of cows? While some may recognize that this system for artificial insemination has some utility in agriculture and might even potentially be of vital importance to humans who can conceive by no other means, others may regard it as morally or ethically unacceptable. Thus, in addition to the good, practical considerations that arise in designing and implementing a new system, moral and ethical concerns may also need to be considered for certain applications. Even if the appropriate “wise” function is not actually incorporated in a given device or system, one would hope that the wisdom of the designer(s) would ultimately prevail in situations where such issues apply.

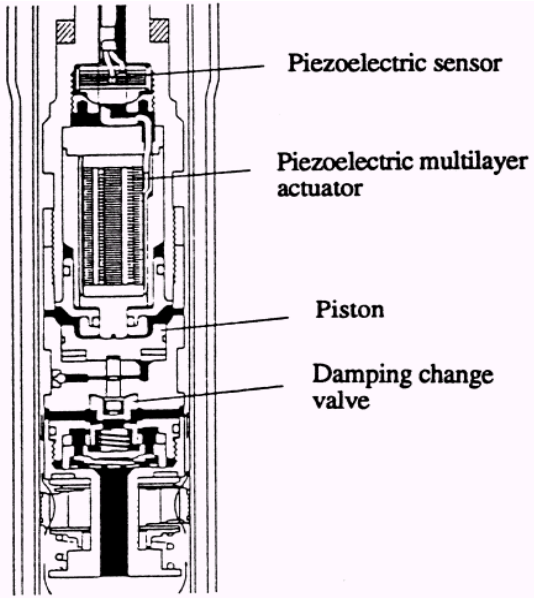


**Figure 32** An electronic modulated automobile shock absorber developed by Toyota Motors using a both a multilayer piezoelectric sensor and actuator.<sup>31</sup>

## REFERENCES

- 1) I. Inazaki: *Sensor Technology* **2**, No.2, 65 (1982).
- 2) K. Uchino: *Ultrasonic Techno*, No. 8, 19 (1993).
- 3) *Optical Spectra*, March, p.46 (1979).
- 4) S. Moriyama: *Mechanical Design* **27**, No.1, 32 (1983).
- 5) U. Berg, M. Begemann, B. Hagemann, K.-P. Kamper, F. Michel, C. Thurigen, L. Weber and Th. Wittig: *Proc. 6<sup>th</sup> Int'l Conf. New Actuators*, p.552 (1998).
- 6) J. Bryzek, K. Petersen and W. McCulley: *IEEE Spectrum*, No. 5, p.20 (1994).
- 7) S. Egawa, T. Niino and T. Higuchi: *Proc. 1991 IEEE Workshop on Micro Electro Mechanical Systems*, p.9 (1991).
- 8) T. Higuchi: *New Actuator Handbook for Precision Control*, p.182, Fuji Techno System, Tokyo (1994).
- 9) H. Horikawa and K. Otsuka: *New Actuator Handbook for Precision Control*, p.454, Fuji Techno System, Tokyo (1994).
- 10) K. Otsuka and C. M. Wayman: *Shape Memory Materials*, Chap.1, p.1, Cambridge University Press, UK (1998).
- 11) K.N. Nelton: *Shape Memory Materials*, Chap.10, Cambridge Univ. Press, UK (1998).
- 12) T. Todoroki, K. Fukuda and T. Hayakumo: *Industrial Materials*, **32**, No.7, 85 (1984).
- 13) A. B. Flatau, M. J. Dapino and F. T. Calkins: *Magnetostrictive Composites*, *Comprehensive Composite Materials*, Chapter 5.26, p.563 (2000).
- 14) A. E. Clark and H. S. Belson: US Patent 4,378,258 (1983).
- 15) H. Eda: *Giant Magnetostrictive Actuators*, *New Actuator Handbook for Precision Control*, p.90, Fuji Techno System, Tokyo (1994).
- 16) J. L. Butler: Edge Technologies, Ames, IA (1988).
- 17) K. Uchino: *Ferroelectric Devices*, p.11, Marcel Dekker, NY (2000).
- 18) K. Yano, T. Hamatsuki, I. Fukui and E. Sato: *Proc. Annual Mtg. EE Japan*, p.1-157 (Spring, 1984).
- 19) M. Kasuga, T. Satoh, N. Tsukada, T. Yamazaki, F. Ogawa, M. Suzuki, I. Horikoshi and T. Itoh: *J. Soc. Precision Eng.*, **57**, 63 (1991).
- 20) V. Bharti, H.S. Xu, G. Shanti, Q.M. Zhang and K. Liang: *J. Appl. Phys.* **87**,452 (2000).
- 21) S. Bauer: *Proc. Int'l Symp. Smart Actuators*, ICAT/Penn State, PA (April, 1999).
- 22) K. Uchino: *Mat. Res. Innovat.*, **1**, 163 (1997).
- 23) M. Tanimura and K. Uchino: *Sensors and Mater.*, **1**, 47 (1988).
- 24) K. Uchino: *J. Rob. Mech.*, **1**(2), 124 (1989).
- 25) S. Thakoor, J. M. Morookian, and J. A. Cutts: *Conf. Proc. 10th IEEE Int'l Symp. on Appl. Ferroelectrics*, **1**, 205 (1996).
- 26) P. Poosanaas, K. Tonooka, and K. Uchino, *Mechatronics* **10**, 467 (2000).
- 27) M. R. Jolly and J. D. Carlson: *Composites with Field-Responsive Rheology*, *Comprehensive Composite Materials*, Chapter 5.27, p.575 (2000).
- 28) T. Shiga, A. Okada and T. Kurauchi: *Macromolecules*, **26**, 6958 (1993).
- 29) V. D. Chase: *Appliance Manufacturer*, May, p.6 (1996).
- 30) J. D. Carlson and K. D. Weiss: US Patent 5,382,373 (1995).
- 31) Y. Yokoya: *Electronic Ceramics* **22**, No.111, 55 (1991).

The following review papers and books are recommended for further study:

- 32) K. Uchino: *Piezoelectric/Electrostrictive Actuators*, Morikita Publishing, Tokyo (1986).
- 33) K. Uchino: *Ceramic Actuators: Principles & Applications*, *MRS Bull.* **18**(4), 42 (1993).
- 34) S. Ueha, Y. Tomikawa, M.Kurosawa and N.Nakamura: *Ultrasonic Motors: Theory and Applications*, Oxford Science Publ., Monographs in EE. Eng. 29 (1993).
- 35) K. Uchino: *Ferroelectric Devices*, VCH, Materials Sci. and Tech. Vol.11, Chap.12 (1994).
- 36) K. Uchino: *Proc. Electroceramics IV*, Vol.1, p.179, RWTH, Aachen (1994).
- 37) K. Uchino: *Piezoelectric Actuators and Ultrasonic Motors*, Kluwer Academic Publishers, MA (1996).
- 38) K. Uchino: *Ferroelectric Devices*, Marcel Dekker, NY (2000).